Protochlorophyllide Oxidoreductase: "Dark" Reactions of a Light-Driven Enzyme[†]

Derren J. Heyes,* Alexander V. Ruban, and C. Neil Hunter

Robert Hill Institute for Photosynthesis and Krebs Institute for Biomolecular Research, Department of Molecular Biology and Biotechnology, University of Sheffield, Sheffield S10 2TN, United Kingdom

Received September 12, 2002; Revised Manuscript Received November 20, 2002

ABSTRACT: The light-driven enzyme NADPH:protochlorophyllide oxidoreductase (POR) catalyzes the reduction of protochlorophyllide (Pchlide) to chlorophyllide (Chlide), a key regulatory step in the chlorophyll biosynthesis pathway. As POR is light activated, it allows intermediates in the reaction pathway to be observed by initiating catalysis with illumination at low temperatures, a technique that has recently been used to study the initial photochemistry. Here, we use low-temperature spectroscopy to show that the catalytic mechanism of POR involves two additional steps, which do not require light and have been termed the "dark" reactions. The first of these involves the conversion of the product of the initial light-driven reaction, a nonfluorescent radical species, into a new intermediate that has an absorbance maximum at 681 nm and a fluorescence peak at 684 nm. During the second dark step this species gradually blue shifts to yield the product, Chlide. The temperature dependence for each of these two processes was measured; the data revealed that these steps could only occur close to or above the "glass transition" temperature of proteins, suggesting that domain movements and/or reorganization of the protein are required for these stages of the catalytic mechanism.

Within the chlorophyll biosynthetic pathway the reduction of the C17−C18 double bond of the D-ring of protochlorophyllide (Pchlide)[1] to produce chlorophyllide (Chlide) is catalyzed by the light-driven enzyme NADPH:protochlorophyllide oxidoreductase (POR; EC 1.3.1.33) (*1*). As a result of its requirement for light POR is crucial to the assembly of the photosynthetic apparatus and subsequent plant growth and development (*2*).

Comparisons of the amino acid sequence of POR with other sequences in the database led to the conclusion that POR is a member of the "RED" superfamily of enzymes (*r*eductases, *e*pimerases, *d*ehydrogenases) (*3*, *4*). The majority of enzymes in this large protein family catalyze NADP(H)- or NAD(H)-dependent reactions involving hydride and proton transfers and are generally homodimers or homotetramers (*5*). The crystal structures of several members of the family have been determined (for example, see refs *6* and *7*) and have subsequently been used as a template to produce a homology model of POR (*8*). Throughout this family several features have been retained, including conserved cofactor binding domains in the N-terminal half of the protein and highly conserved Tyr and Lys residues, which have been shown to be essential for POR activity (*5*, *8*−*10*). Hence, all of the members of the RED family are suggested to have similar mechanisms of catalysis. The experimental advantages of studying POR may lead to this enzyme serving as an important generic model for understanding the mechanism of catalysis by the RED family.

Although the reaction catalyzed by POR has been extensively studied, the catalytic mechanism remains largely unresolved. Studies with cofactor analogues have revealed that NADPH is absolutely essential for the photoreduction (*1*), and upon binding to the enzyme it protects one or more of the conserved Cys residues in the protein from chemical modification (*11*, *12*). Furthermore, by using 4*R* and 4*S* ^{3}H-radiolabeled isomers of NADPH, it has been shown that the hydride is transferred from the *pro-S* face of the nicotinamide ring to the C17 position of the Pchlide molecule (*13*, *14*). It has been proposed that the conserved Tyr donates a proton to the C18 position (Figure 1) whereas the close proximity of the Lys residue is thought to be necessary to lower the apparent pK_a of the phenolic group of the Tyr, allowing deprotonation to occur (*4*). In addition, changes to the central Mg atom (*15*) and to the structure of the isocyclic ring of the Pchlide molecule lead to POR inactivity (*16*), suggesting that these structural elements are also important for the interaction of the pigment with the enzyme. Etioplast membranes have often been used to study different spectroscopic forms of Pchlide and Chlide (*17*−*21*), but several processes, such as POR aggregation and prolamellar body formation (*22*), can complicate the study of Pchlide photoreduction in these preparations. However, the use of heterologously expressed POR has provided an excellent opportunity to study the reaction mechanism in greater detail (*9*, *11*, *23*−*26*). For example, recombinant PORs from barley, pea, and *Synechocystis* have recently been used to identify intermediates in the reaction (*9*, *25*, *26*).

Along with DNA photolyase (*27*) POR is the only other enzyme studied so far that exhibits a requirement for light.

[†] This work was supported by the Joint Infrastructure Fund and the Biotechnology and Biological Sciences Research Council, U.K.

* To whom correspondence should be addressed at the Department of Molecular Biology and Biotechnology, University of Sheffield, Firth Court, Western Bank, Sheffield S10 2TN, U.K. Tel: +44 (0)114 2224240. Fax: +44 (0)114 2222711. E-mail: d.j.heyes@shef.ac.uk.

[1] Abbreviations: Chlide, chlorophyllide; fwhm, full width at half-maximum; Pchlide, protochlorophyllide; POR, NADPH:protochlorophyllide oxidoreductase; RED, reductases, epimerases, dehydrogenases; SDS, sodium dodecyl sulfate.

10.1021/bi0268448 CCC: $25.00
Published on Web 12/21/2002

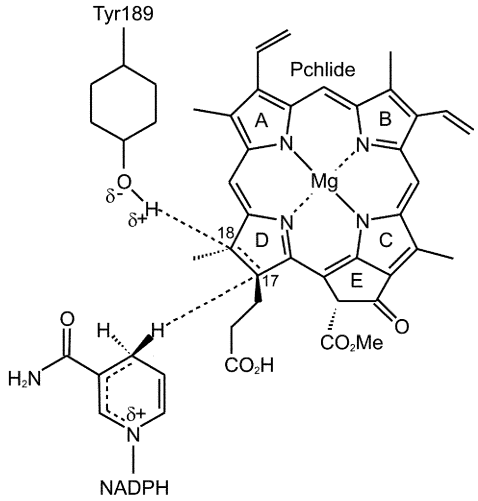

FIGURE 1: Proposed mechanism of catalysis by POR. The proton at the C18 position of Pchlide is derived from Tyr189, and the hydride transferred to the C17 position is derived from the *pro-S* face of NADPH.

The light dependence of the catalytic mechanism of POR therefore offers an exciting opportunity to gain new information on how the free energy of a photon can be harnessed to power enzyme catalysis. Furthermore, catalysis can be initiated by illuminating active POR−NADPH−Pchlide complexes at low temperatures to trap intermediates in the reaction pathway. We recently used this approach to study the initial photochemistry in the POR-catalyzed reaction, which can occur below 200 K (*26*). This step involves the formation of a nonfluorescent intermediate with a broad absorbance band at 696 nm (A_{696}) that is suggested to represent an ion radical complex. In the present work the subsequent nonphotochemical or "dark" events prior to Chlide formation have been analyzed by using low-temperature fluorescence and absorbance spectral measurements. We have identified two such dark steps and have carried out a thorough examination of the temperature dependence of each.

MATERIALS AND METHODS

Expression and Purification of Synechocystis POR. His-tagged POR from *Synechocystis* sp. PCC6803 was overproduced in *Escherichia coli* and purified as previously described (*11*). The enzyme was purified further on a second column (2.5 cm × 10 cm) containing Red Sepharose CL-6B (Pharmacia Biotechnology) equilibrated with 50 mM Tris-HCl (pH 7.5), 1 mM DTT, and 20 mM NaCl. The resin was washed with 10−20 column volumes of this buffer, and the His-tagged POR was eluted with 50 mM Tris-HCl (pH 7.5), 1 mM DTT, and 1 M NaCl. Protein concentrations were determined using the Bio-Rad DC protein assay with bovine serum albumin (BSA) as standard.

Pchlide Preparation. Pchlide was isolated from *Rhodobacter capsulatus* ZY5 cultures grown in RCV$^+$ medium (*28*) containing 25 μg/μL rifampicin in the dark at 32 °C. This strain has a mutation in one of the three subunits required for the light-independent reduction of Pchlide, which results in the accumulation of the pigment. During growth, Pchlide was released into the medium and adsorbed onto polyurethane foam bungs. The pigment was extracted from the bungs into 100% ice-cold acetone and passed down a CM-Sepharose column (2.5 cm × 10 cm, Sigma) equilibrated with 100% acetone. Contaminating pigments were removed with 5% methanol/95% acetone, and Pchlide was eluted with 25% methanol/75% acetone. This was then dried under nitrogen and stored in the dark at −20 °C until required. Before use, the pigment was redissolved in 100% methanol.

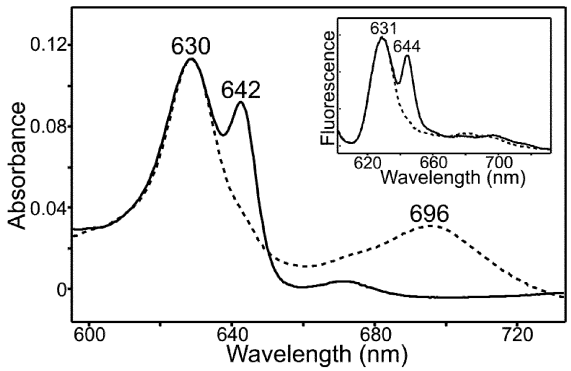

FIGURE 2: Formation of the nonfluorescent intermediate, A_{696}, measured by low-temperature spectroscopy. 77 K absorbance spectra of samples containing 3.9 μM Pchlide, 60 μM POR, and 200 μM NADPH before (solid line) and after (dashed line) illumination for 10 min at 180 K. The inset shows 77 K fluorescence emission spectra of samples containing 1 μM Pchlide, 33 μM POR, and 130 μM NADPH before (solid line) and after (dashed line) illumination for 10 min at 180 K. Spectra were recorded with an excitation wavelength of 430 nm and were normalized to the fluorescence of 0.5 μM fluorescein at 500 nm.

Low-Temperature Spectroscopic Characterization of the Dark Reactions. Samples in activity buffer [60% sucrose, 50 mM Tris-HCl (pH 7.5), 100 mM NaCl, 0.1% (v/v) Genapol X-080, 0.1% (v/v) β-mercaptoethanol] were maintained at the required temperature using an OpstistatDN nitrogen bath cryostat (Oxford Instruments). The temperature of the sample was monitored directly with a thermocouple sensor (Comark). The first light-dependent step in the reaction was initiated by illuminating samples for 10 min at 180 K by using a Schott KL1500 electronic cold light source (1500 μmol m^{-2} s^{-1} white light). The samples were then warmed and maintained for 10 min at gradually higher temperatures in the dark. All fluorescence emission and excitation spectra were recorded using a SPEX FluoroLog spectrofluorimeter (Jobin Yvon Ltd.) at 77 K. The exciting light was provided from a xenon light source, excitation monochromator slit widths were 4.5 nm, and emission monochromator slit widths were 3.6 nm. Absorbance spectra were recorded with a Cary 500 Scan UV−visible−NIR (Varian) spectrophotometer at 77 K. Normalization of the spectra, spectral deconvolutions, and difference spectra were calculated using the GRAMS/32 software.

RESULTS

We have previously demonstrated that the initial photochemical reaction in the reduction of Pchlide can occur below 200 K (*26*) and that it involves the formation of a stable nonfluorescent intermediate with a broad absorbance band at 696 nm (A_{696}). To identify further intermediates in the reaction pathway, it was first necessary to form this intermediate by illuminating all samples at 180 K for 10 min. Fluorescence and absorbance spectra, measured at 77 K, subsequently confirmed that formation of the nonfluorescent A_{696} state had occurred (Figure 2). These samples were then

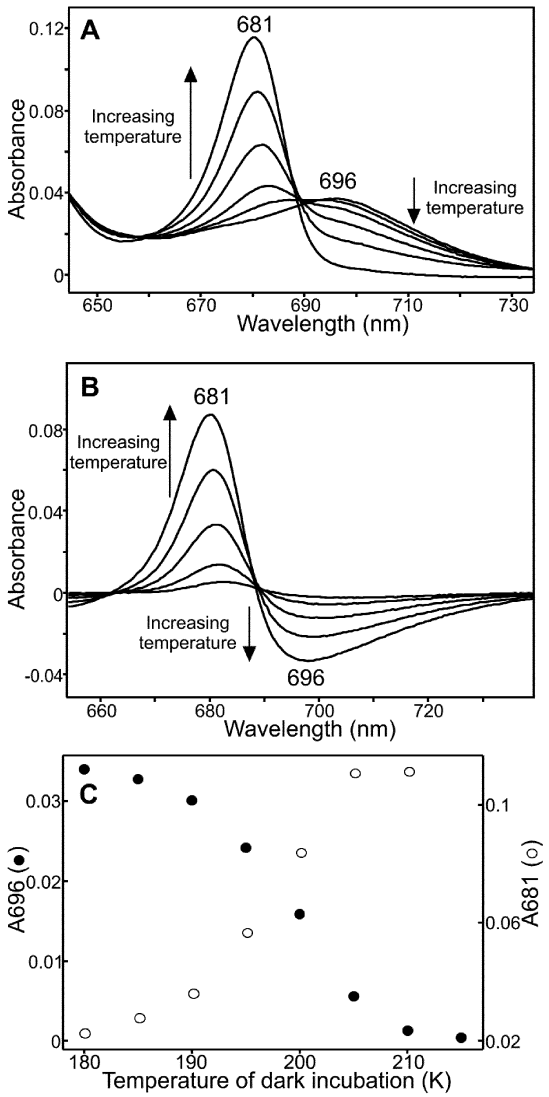

FIGURE 3: Characterization of the first dark step by low-temperature absorbance measurements. (A) 77 K absorbance spectra of samples containing 3.9 μM Pchlide, 60 μM POR, and 200 μM NADPH after incubation in the dark for 10 min at increasing temperatures. Samples were incubated at 180, 185, 190, 195, 200, and 205 K, respectively. The formation of the absorbance peak at 681 nm and simultaneous disappearance of the broad absorbance band at 696 nm at higher temperatures are indicated by the arrows. (B) Difference spectra of samples from (A) using the sample that was illuminated at 180 K as a blank. The arrows clearly show the increase in A_{681} and decrease in A_{696} at elevated temperatures. (C) The temperature dependence of the first nonphotochemical step was obtained by measuring both A_{681} formation (○) and A_{696} disappearance (●).

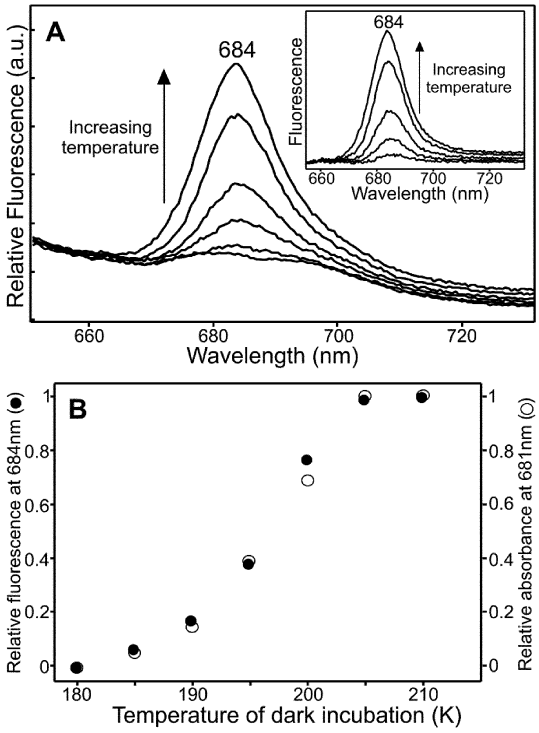

FIGURE 4: The first dark step measured by low-temperature fluorescence emission spectra. (A) 77 K fluorescence emission spectra of samples containing 1 μM Pchlide, 33 μM POR, and 150 μM NADPH after incubation in the dark for 10 min at 180, 185, 190, 195, 200, and 205 K, respectively. The arrow indicates the formation of a fluorescence band at 684 nm at increasing temperatures. Spectra were recorded with an excitation wavelength of 430 nm and were normalized to the fluorescence of 0.5 μM fluorescein at 500 nm. Difference spectra (inset) were measured using the sample that was illuminated at 180 K as a blank. (B) The relative increase in fluorescence at 684 nm (●) was calculated using the fluorescence spectra from (A) over the temperature range 180−205 K. The temperature dependence of A_{681} formation is also overlaid (○).

warmed to progressively higher temperatures in the dark, and as a result two nonphotochemical steps could be observed by low-temperature fluorescence and absorbance measurements.

Spectroscopic Characterization of the First Dark Step. Low-temperature absorbance spectra show that the first dark step involves the disappearance of the broad band at 696 nm together with the simultaneous appearance of a new intermediate absorbing at 681 nm (Figure 3A). The conversion of A_{696} to A_{681} can be seen more clearly upon examination of the difference spectra (Figure 3B). Spectral deconvolution shows that the new peak has a full width at half-maximum (fwhm) of 14 nm (323 cm^{-1}). A temperature dependence of this first nonphotochemical step, where the decrease in A_{696} mirrored the increase in A_{681}, reveals that it can occur between 185 and 205 K (Figure 3C).

The equivalent step was also monitored by using 77 K fluorescence measurements (Figure 4A). The nonfluorescent intermediate, which is formed after the initial photochemical reaction, is converted to a new species with a fluorescence band at 684 nm (F_{684}). Spectral deconvolution of this new band reveals that it consists of a single component with a half-bandwidth of 16 nm (344 cm^{-1}). The temperature dependence of F_{684} formation shows that it occurs in the same temperature range as A_{681} formation (Figure 4B), indicating that both spectral changes belong to the same process.

The Second Dark Step Involves the Production of Chlide. The second nonphotochemical step, which occurs at temperatures above 205 K, appears to be more complex. Absorbance spectra at 77 K show that the 681 nm absorbing species gradually blue shifts, and at temperatures above 260 K this eventually leads to the formation of Chlide with a characteristic absorbance band at 671 nm (Figure 5A). Deconvolution of this 671 nm peak confirms that it is a single component with a fwhm of 18 nm (401 cm^{-1}). A number of species were detected after dark incubation at temperatures between 205 K and room temperature, with absorbance maxima at intermediate wavelengths between 671 and 681

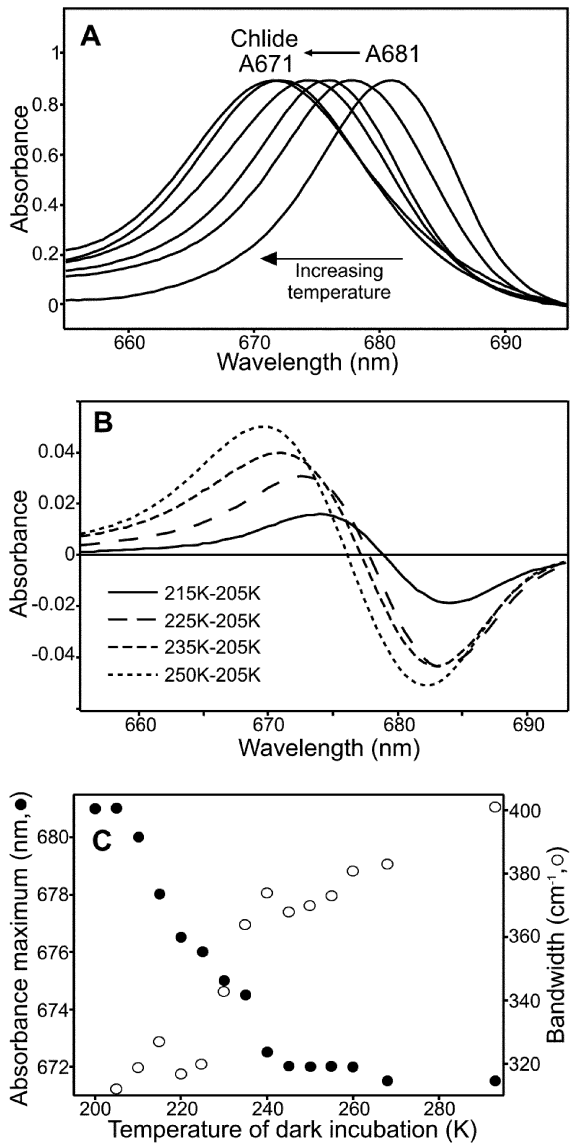

FIGURE 5: The final step in Pchlide photoreduction involves a blue shift of A_{681} to produce Chlide. (A) 77 K absorbance spectra of samples containing 3.9 μM Pchlide, 60 μM POR, and 200 μM NADPH after incubation in the dark for 10 min at 205, 215, 225, 235, 250, and 293 K, respectively. The arrow signifies spectra measured at increasing temperatures. (B) Difference spectra of samples from (A) after incubation at 215, 225, 235, and 250 K, respectively. The sample that had been incubated in the dark for 10 min at 205 K was used as a blank. (C) A plot of the absorbance wavelength maximum against the temperature of dark incubation yields a temperature dependence for the second dark step (●). The fwhm for each species has also been calculated in wavenumbers (○).

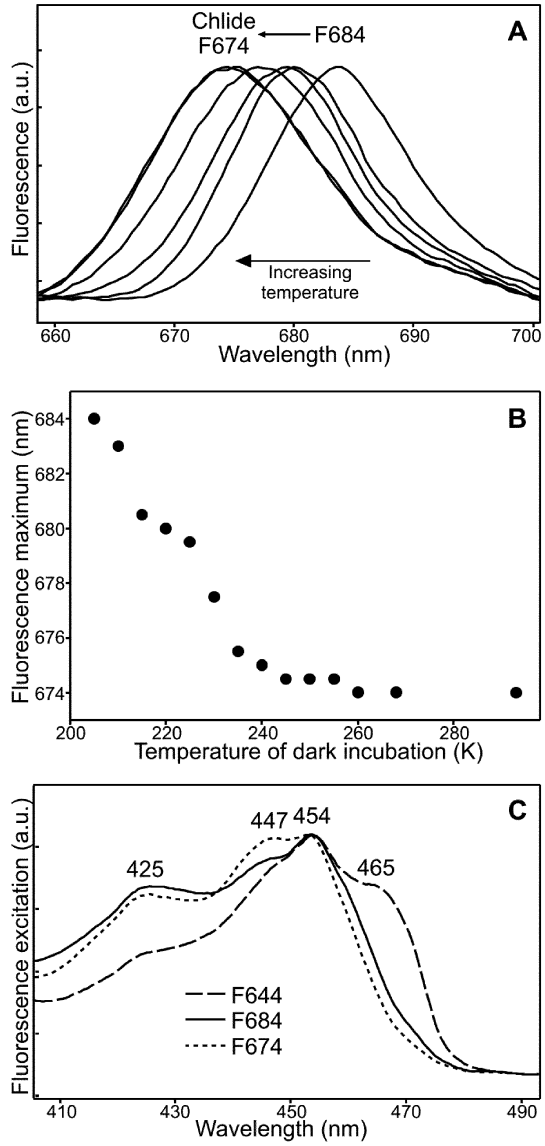

FIGURE 6: The second dark step monitored by low-temperature fluorescence measurements. (A) 77 K fluorescence emission spectra of samples containing 1 μM Pchlide, 33 μM POR, and 150 μM NADPH after incubation in the dark for 10 min at 205, 215, 225, 235, 250, and 293 K, respectively. Spectra were recorded with an excitation wavelength of 430 nm and were normalized to the fluorescence of 0.5 μM fluorescein at 500 nm. The arrow shows that F_{684} blue shifts at higher temperatures to produce a fluorescence band at 674 nm, representing Chlide. (B) The temperature dependence of the second dark step was calculated by measuring the fluorescence wavelength maximum at each point. (C) 77 K fluorescence excitation spectra of the 644, 684, and 674 nm emission bands of a sample containing 1 μM Pchlide, 33 μM POR, and 150 μM NADPH.

nm. At first glance it would appear that these states are simply a mixture of two species, caused by the loss of the 681 nm band and simultaneous formation of the 671 nm band. However, second derivatives, spectral deconvolution, and difference spectra reveal that these peaks all consist of a single component (Figure 5B). This is clearly indicated by the fact that there is no isosbestic point, which is in contrast to the spectra from Figure 3. As the temperature of incubation increases, the fwhm of the bands also increases from 14 to 18 nm. Hence, the second dark step in the reaction can be represented by a progressive blue shift of the 681 nm band to produce the final product, Chlide. The wavelength maximum and fwhm of each species can be plotted to yield a temperature dependence of this final step in the reaction (Figure 5C).

A similar effect is observed when the same step is studied by using low-temperature fluorescence measurements. The intermediate that fluoresces at 684 nm gradually blue shifts to produce Chlide, which has a fluorescence peak at 674 nm (Figure 6A). Furthermore, the fwhm of the band increases from 16 nm for F_{684} to 20 nm (432 cm^{-1}) for F_{674}. The temperature dependence of this step, which is obtained by monitoring the fluorescence wavelength maximum, shows

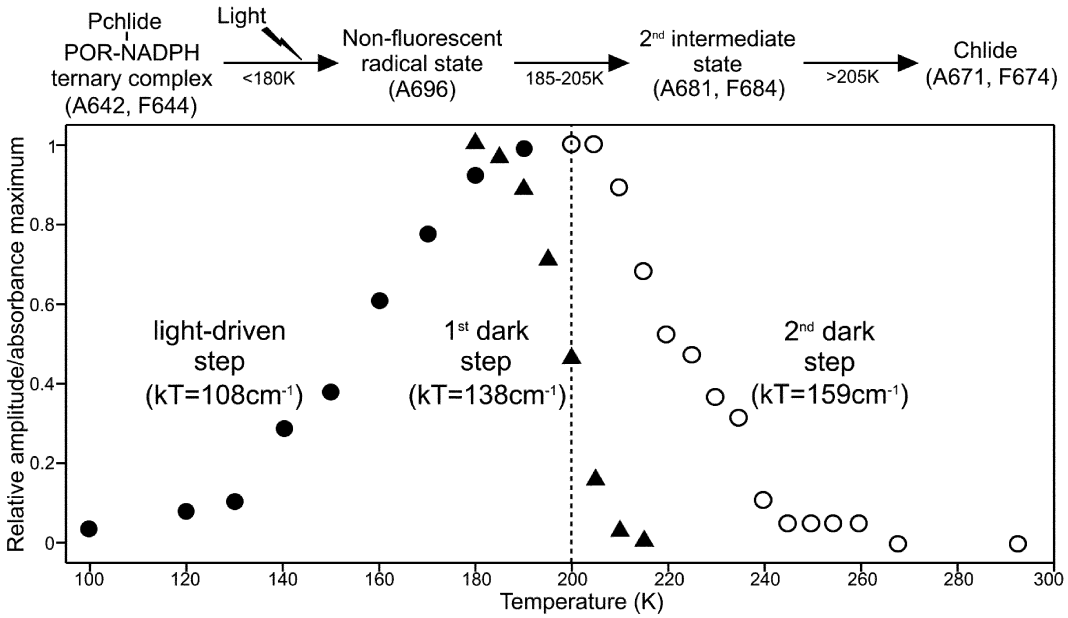

FIGURE 7: Overall scheme of the steps involved in the POR-catalyzed reaction. One light-driven step (*26*) and two dark steps have been identified using low-temperature spectroscopy. The temperature dependence is shown together with the *kT* value for each step, where *k* is the Boltzmann constant (0.695 cm^{-1}) and *T* is the midpoint temperature of each process. The glass transition temperature of proteins is also shown as a reference (dashed line).

that it can occur between 205 K and room temperature (Figure 6B), in agreement with the absorbance data.

Excitation Spectra of Pchlide and Chlide States. To further emphasize the different spectral properties of the various states, Figure 6C shows the excitation spectra of the initial POR−NADPH−Pchlide ternary complex (F_{644}), the second intermediate in the reaction (F_{684}), and the final product, Chlide (F_{674}). The F_{644} band has two main excitation maxima at 454 and 465 nm whereas the F_{674} band has three excitation peaks at 425, 447, and 454 nm, respectively. The excitation spectrum of the F_{684} intermediate is very similar to that of the F_{674} band, with the three excitation peaks in identical positions.

DISCUSSION

The POR-catalyzed photoreduction of Pchlide to produce Chlide is a crucial reaction in the chlorophyll biosynthetic pathway. POR is a member of the large RED family of enzymes (*5*), all of which are suggested to have similar mechanisms of catalysis, involving hydride and proton transfer. Moreover, the unique light dependence of the enzyme makes it an attractive model for studying the mechanism of this family and more generally biological proton and hydride transfers. The enzyme−substrate complex can be formed without triggering any catalytic activity, and intermediates in the reaction pathway can subsequently be trapped by illumination at low temperatures.

The initial photochemical step in the reaction involves the formation of a nonfluorescent intermediate with a broad absorbance band at 696 nm (A_{696}), which was proposed to represent a radical state (*26*). No product state was observed after this first light-driven step, implying that it must be followed by one or more dark steps. In the present work heterologously expressed POR from *Synechocystis* (*11*) has been used to characterize the subsequent dark steps. By using a combination of low-temperature fluorescence and absorbance measurements, we have identified two nonphotochemical reactions, each of which has a distinct temperature dependence.

The first dark step involves the conversion of the nonfluorescent radical state, with a broad absorbance maximum at 696 nm, into a new intermediate that has a much narrower absorbance band centered at 681 nm. When the same step is studied using fluorescence measurements, the new species was found to have a fluorescence band at 684 nm. Both of these spectral changes were shown to have an identical temperature dependence, occurring between 185 and 205 K, which provides thermodynamic evidence that they belong to the same pigment state. The second dark process and next step in the reaction involves a gradual blue shift and broadening of the absorbance band at 681 nm to yield the final product, Chlide (A_{671}). The same phenomenon is observed in the fluorescence spectra with a blue shifting of the F_{684} band to yield Chlide and a characteristic fluorescence band at 674 nm. This final step in the reaction pathway only occurs at temperatures above 205 K. Therefore, three essential steps in the photoreduction of Pchlide to Chlide can be identified by using low temperatures in different ranges to separate the reactions. This is fortuitous and occurs because the temperature domains over which these three steps occur do not overlap significantly. Figure 7 illustrates this point and includes data from a previous temperature dependence study of the initial light-driven step (*26*).

At around 200 K proteins undergo a dynamic transition, termed the "glass transition", below which all protein motions are frozen out (*29*−*31*). Therefore, conformational changes in the protein cease below 200 K, and for the majority of enzymes this results in loss of enzymatic activity. In the POR-catalyzed reduction of Pchlide the photochemistry can still proceed well below 200 K, demonstrating that domain movements or reorganization of the enzyme are not involved at this stage of the catalytic mechanism. Conversely, the

ensuing first dark step occurs at temperatures close to the glass transition and may therefore involve protein motions (Figure 7). Moreover, the final step in the reaction pathway can only proceed at temperatures greater than 200 K, suggesting that this stage of catalysis is assisted by the participation of domain movements and/or reorganization of the enzyme. The second dark step occurs over a much wider temperature range than the first dark step, and this could arise from the different reaction mechanisms involved.

An intermediate similar to $A_{681}-F_{684}$, with a fluorescence band at 682 nm, was recently identified *in vitro* as being the product of an initial photochemical reaction (*9*, *25*). However, we have now shown that this species is in fact the second intermediate in the reduction of Pchlide and is the product of the first dark reaction. Although the exact molecular nature of the intermediate is not known at this time, it has a fluorescence excitation spectrum very similar to that of the final product, Chlide. It is interesting to note that comparable Chlide species, with fluorescence maxima at 684 nm, have been detected in etioplast membranes (*17*, *20*). These have been suggested to represent a POR−$NADP^+$−Chlide complex with the $A_{671}-F_{674}$ species corresponding to "free" or unbound Chlide (*20*). If this is applied to our system, then $A_{681}-F_{684}$ may represent a POR−$NADP^+$−Chlide complex that can be formed directly from the nonfluorescent state. At higher temperatures the Chlide could then be released from the enzyme to yield the unbound product. However, as we could not see a mixture of A_{681} and A_{671} forms at intermediate temperatures, it is more likely that the majority of the spectra arise from the Chlide molecule still bound to the same locus as the A_{681} form. At successively higher temperatures in the 205−293 K region the low-frequency protein modes will become enhanced; this could gradually affect the binding strength of Chlide and $NADP^+$, as well as the interaction between these products. We have already demonstrated that in the POR−NADPH−Pchlide ternary complex the Pchlide absorbance is red shifted by ∼13 nm (*26*). It is possible that the blue shifts we observe here reflect the opposite process, a gradual dissolution of the POR−$NADP^+$−Chlide ternary product complex. This process, as well as causing a gradual blue shift, could contribute to the progressive inhomogeneous broadening of the absorption spectrum. The temperature range over which the blue shift and broadening occur, 205−293 K, corresponds to an energy difference of ∼60 cm^{-1}. It is possible that the increase in thermal energy is conserved by the POR−$NADP^+$−Chlide complex and is directly reflected in the increased bandwidth of the Chlide molecule (∼80 cm^{-1}), as opposed to being conserved by the low-frequency modes in the enzyme or $NADP^+$. The conservation of this energy in the bound Chlide molecule is emphasized by the fact that all of the absorbance and fluorescence spectra in Figures 5 and 6 were recorded at the same temperature (77 K). Thus, the A_{681} form is transformed from being in a "rigid" binding site into an A_{671} form in a partially "relaxed" binding locus. Interestingly, we do not observe either of the long-wavelength intermediates, F_{690} or F_{696}, which have been observed in etioplast membranes and have been suggested to represent a POR−NADPH−Chlide complex (*17*, *20*).

Hence, we have shown that the essential steps in the photoreduction of Pchlide can be monitored by triggering the reaction at low temperatures. Furthermore, the mechanism of catalysis by POR, involving coupled proton and hydride transfer, consists of three steps: a light-driven one occurring below 200 K, followed by two dark steps in which catalysis is assisted by nuclear protein motions. This information will aid an understanding of the mechanisms and temperature domains of hydride and proton transfers in biological systems.

REFERENCES

1. Griffiths, W. T. (1978) *Biochem. J. 174*, 681−692.
2. Lebedev, N., and Timko, M. P. (1998) *Photosynth. Res. 58*, 5−23.
3. Baker, M. E. (1994) *Biochem. J. 300*, 605−607.
4. Wilks, H. M., and Timko, M. P. (1995) *Proc. Natl. Acad. Sci. U.S.A. 92*, 724−728.
5. Jörnvall, H., Persson, B., Krook, M., Atrian, S., Gonzalez-Duarte, R., Jeffery, J., and Ghosh, D. (1995) *Biochemistry 34*, 6003−6013.
6. Tanaka, N., Nonaka, T., Nakanishi, M., Deyashiki, Y., Hara, A., and Mitsui, Y. (1996) *Structure 4*, 33−45.
7. Tanaka, N., Nonaka, T., Tanabe, T., Yoshimoto, T., Tsuru, D., and Mitsui, Y. (1996) *Biochemistry 35*, 7715−7730.
8. Townley, H. E., Sessions, R. B., Clarke, A. R., Dafforn, T. R., and Griffiths, W. T. (2001) *Proteins 44*, 329−335.
9. Lebedev, N., Karginova, O., McIvor, W., and Timko, M. P. (2001) *Biochemistry 40*, 12562−12574.
10. Heyes, D. J., and Hunter C. N. (2002) *Biochem. Soc. Trans. 30*, 601−604.
11. Heyes, D. J., Martin, G. E., Reid, R. J., Hunter, C. N., and Wilks, H. M. (2000) *FEBS Lett. 483*, 47−51.
12. Oliver, R. P., and Griffiths, W. T. (1981) *Biochem. J. 195*, 93−101.
13. Valera, V., Fung, M., Wessler, A. N., and Richards, W. R. (1987) *Biochem. Biophys. Res. Commun. 148*, 515−520.
14. Begley, T. P., and Young, H. (1989) *J. Am. Chem. Soc. 111*, 3095−3096.
15. Griffiths, W. T. (1980) *Biochem. J. 186*, 267−278.
16. Klement, H., Helfrich, M., Oster, U., Schoch, S., and Rudiger, W. (1999) *Eur. J. Biochem. 265*, 862−874.
17. Boddi, B., Ryberg, M., and Sundqvist, C. (1991) *Photochem. Photobiol. 53*, 667−673.
18. Boddi, B., Ryberg, M., and Sundqvist, C. (1992) *J. Photochem. Photobiol., B 12*, 389−401.
19. Boddi, B., Ryberg, M., and Sundqvist, C. (1993) *J. Photochem. Photobiol., B 21*, 125−133.
20. Boddi, B., and Franck, F. (1997) *J. Photochem. Photobiol., B 41*, 73−82.
21. Belyaeva, O. B., Timofeev, K. N., and Litvin, F. F. (1988) *Photosynth. Res. 15*, 247−256.
22. Sundqvist, C., and Dahlin, C. (1997) *Physiol. Plant. 100*, 748−759.
23. Martin, G. E. M., Timko, M. P., and Wilks, H. M. (1997) *Biochem. J. 325*, 139−145.
24. Townley, H. E., Griffiths, W. T., and Nugent, J. P. (1998) *FEBS Lett. 422*, 19−22.
25. Lebedev, N., and Timko, M. P. (1999) *Proc. Natl. Acad. Sci. U.S.A. 96*, 9954−9959.
26. Heyes, D. J., Ruban, A. V., Wilks, H. M., and Hunter, C. N. (2002) *Proc. Natl. Acad. Sci. U.S.A. 99*, 11145−11150.
27. Aubert, C., Vos, M. H., Mathis, P., Eker, A. P., and Brettel, K. (2000) *Nature 405*, 586−590.
28. Biel, A. J., and Marrs, B. L. (1983) *J. Bacteriol. 156*, 686−694.
29. Vitkup, D., Ringe, D., Petsko, G. A., and Karplus, M. (2000) *Nat. Struct. Biol. 7*, 34−38.
30. Teeter, M. M., Yamano, A., Stec, B., and Mohanty, U. (2001) *Proc. Natl. Acad. Sci. U.S.A. 98*, 11242−11247.
31. Dvorsky, R., Sevcik, J., Caves, L. S. D., Hubbard, R. E., and Verma, C. S. (2000) *J. Phys. Chem. 104*, 10387−10397.

BI0268448